

NANO EXPRESS

Open Access

Strong, conductive carbon nanotube fibers as efficient hole collectors

Yi Jia¹, Xiao Li¹, Peixu Li¹, Kunlin Wang¹, Anyuan Cao², Jinquan Wei¹, Hongwei Zhu^{1,3*} and Dehai Wu^{1*}**Abstract**

We present the photovoltaic properties of heterojunctions made from single-walled carbon nanotube (SWNT) fibers and n-type silicon wafers. The use of the opaque SWNT fiber allows photo-generated holes to transport along the axis direction of the fiber. The heterojunction solar cells show conversion efficiencies of up to 3.1% (actual) and 10.6% (nominal) at AM1.5 condition. In addition, the use of strong, environmentally benign carbon nanotube fibers provides excellent structural stability of the photovoltaic devices.

Keywords: carbon nanotubes, fibers, heterojunction, solar cells

Introduction

As a symbolic nanomaterial, carbon nanotube (CNT) with unique properties like high strength, high electrical conductivity, and chemical inertness has found important applications in optoelectronics [1], being an ideal candidate for various components in photovoltaic devices [2]. CNT bundles can be organized into two typical macrostructures: fibers (1D) and films (2D). The fabrication of homogeneous CNT films with a controllable thickness has been an important basis for the research on CNT-involved devices where CNTs mainly function as transparent electrodes [3]. Our recent work on CNT/Si heterojunction solar cells [4,5] have stimulated a series of studies on the photovoltaic properties of various heterostructures, including CNT/Si [6-16], CNT/CdTe [17], and graphene/Si Schottky junctions [18,19]. Among these devices, the CNT film serves multiple functions as a hole collector, charge transport path, and transparent electrode. However, the CNT film composed of CNT networks has a lot of inter-bundle voids, which should be fairly controlled to achieve high transparency while maintaining sufficient lateral conductivity of the film. The junction resistances between tubes/bundles also yield a limiting value for the conductivities for CNT films [20].

The CNT fiber is yet another macroscopic assembly of CNT bundles in a densified manner. CNT fibers have attracted intensive experimental and theoretical interests and are of increasing practical importance because of their unique 1D structure inherited from individual CNTs [21]. Early research efforts mainly focused on organizing discontinuous nanotubes into ribbon/fiber-like materials. We first reported that long single-walled CNT (SWNT) strands consisting of aligned SWNTs could be synthesized directly with a vertical floating chemical vapor deposition (CVD) method [22]. Many approaches have been developed since then for the assembly of CNTs into continuous fibers through direct spinning [23-26] and post-synthesis spinning [27-30]. Compared to the CNT film, the 1D CNT fiber composed of densely aligned CNT bundles has higher conductance. When forming a heterojunction with silicon, though the fiber itself (generally microns thick) is essentially opaque, the photo-generated charge holes excited from the exposed underlying silicon wafer will transport to it.

The purposes of this work are to introduce the design of the heterojunction solar cells using SWNT fibers as upper electrodes and n-type silicon wafers (n-Si) as photoactive electrodes and to investigate experimentally the photovoltaic properties of the SWNT fiber/Si heterojunctions, verifying the role of SWNTs as hole collectors.

* Correspondence: hongweizhu@tsinghua.edu.cn; wdh-dme@tsinghua.edu.cn

¹Key Laboratory for Advanced Materials Processing Technology, Ministry of Education and Department of Mechanical Engineering, Tsinghua University, Beijing, 100084, People's Republic of China

Full list of author information is available at the end of the article

Experiment

The SWNT fibers used in this study were obtained by a simple film-to-fiber processing reported previously by our group [31]. SWNT films were first prepared by a floating CVD technique with a liquid precursor: a solution of xylene, ferrocene (0.36 mol/L), and sulfur (0.036 mol/L) [32]. Figure 1a shows the as-grown SWNT film hung over a ceramic tray. The film is stiff enough to bear a one-cent-coin weight. The freestanding film is highly transparent and continuous with a large area of approximately 50 cm²; the letters behind can be clearly seen through the film. Highly pure (> 98%) SWNT thin films were then obtained by a two-step posttreatment: hydrogen peroxide oxidation by immersing the films in 30% H₂O₂ solution for 72 h and then rinsing with hydrochloric acid (37% HCl) to remove amorphous impurities and iron catalyst. Smooth and homogenous films could be obtained when ethanol was dropped on the purified samples. A Langmuir monolayer of SWNTs was formed during the spreading of the ethanol layer along the water surface. The film was then picked up slowly with a glass rod (Figure 1b) and allowed to be further densified into a fiber upon drying. As shown in Figure 1c, the fiber was

then twisted under stretching using two motors for 5 to approximately 10 min with a rotating speed of 30 rpm to improve its bulk density and the alignment of the SWNT bundles.

Results and discussion

A scanning electron microscope (SEM) image (Figure 2a) of the SWNT film reveals uniformity of the film across the entire area. Upon twisting, the SWNT fiber became stronger and tougher thanks to the closer contact and improved load transfer between nanotubes due to the enhanced van der Waals forces and friction, which is consistent with previously reported results [27,29,30]. Figure 1d illustrates the strength of a twisted SWNT fiber which sustains a 200-g weight. As further revealed by Figure 2b, d, the SWNT fiber upon twisting became much denser and possessed substantial alignment of the nanotubes along the twisting direction. The fiber diameter was reduced by approximately 35% from 17 to 11 μm. The twist angle, defined as the angle between the longitudinal direction of the SWNT bundles and the axis of the fiber, is about 26°, which is large enough to yield a strong fiber [29]. The result shows that this simple

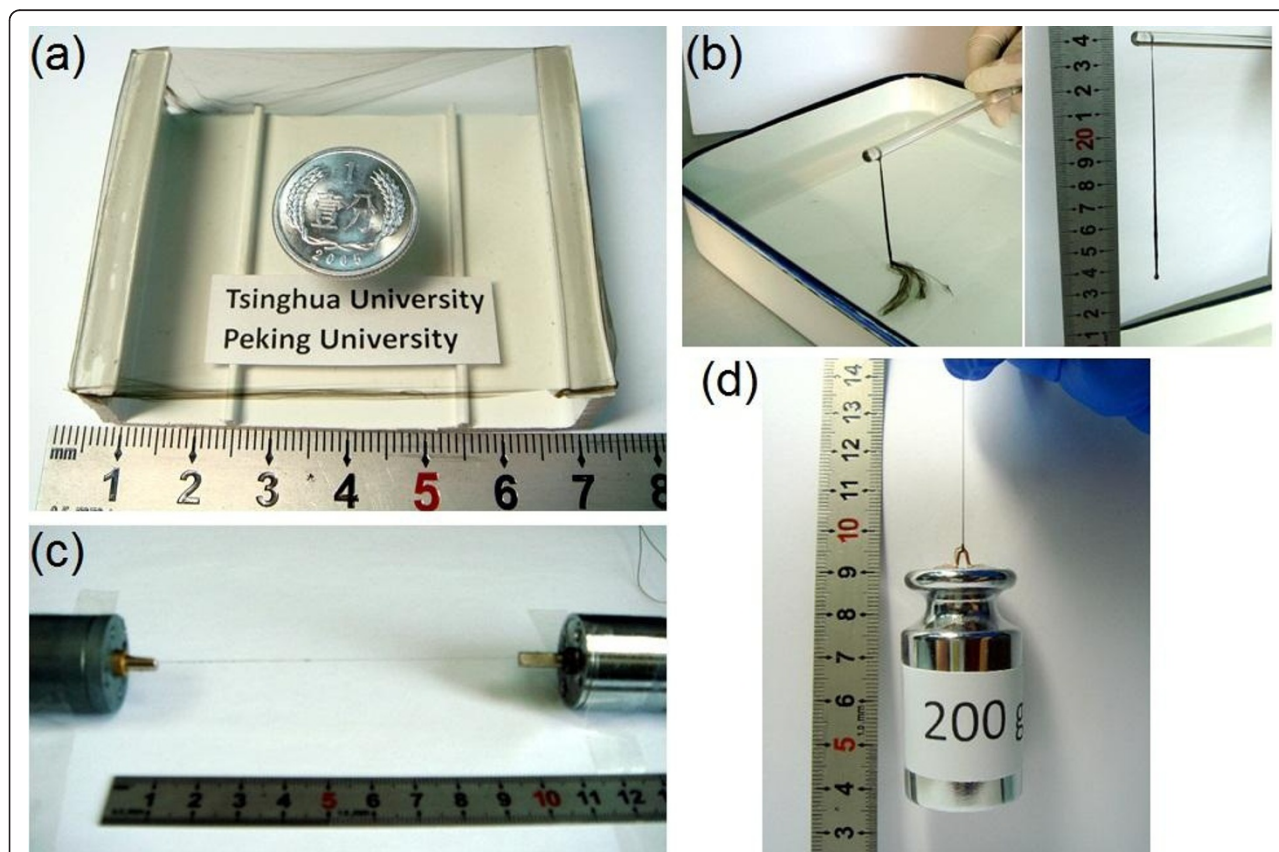


Figure 1 Film-to-fiber processing. (a) Freestanding SWNT thin film with a coin on it. (b) Fiber formation through a wetting/drying process. (c) Fiber twisting. (d) A single fiber bearing a 200-g weight.

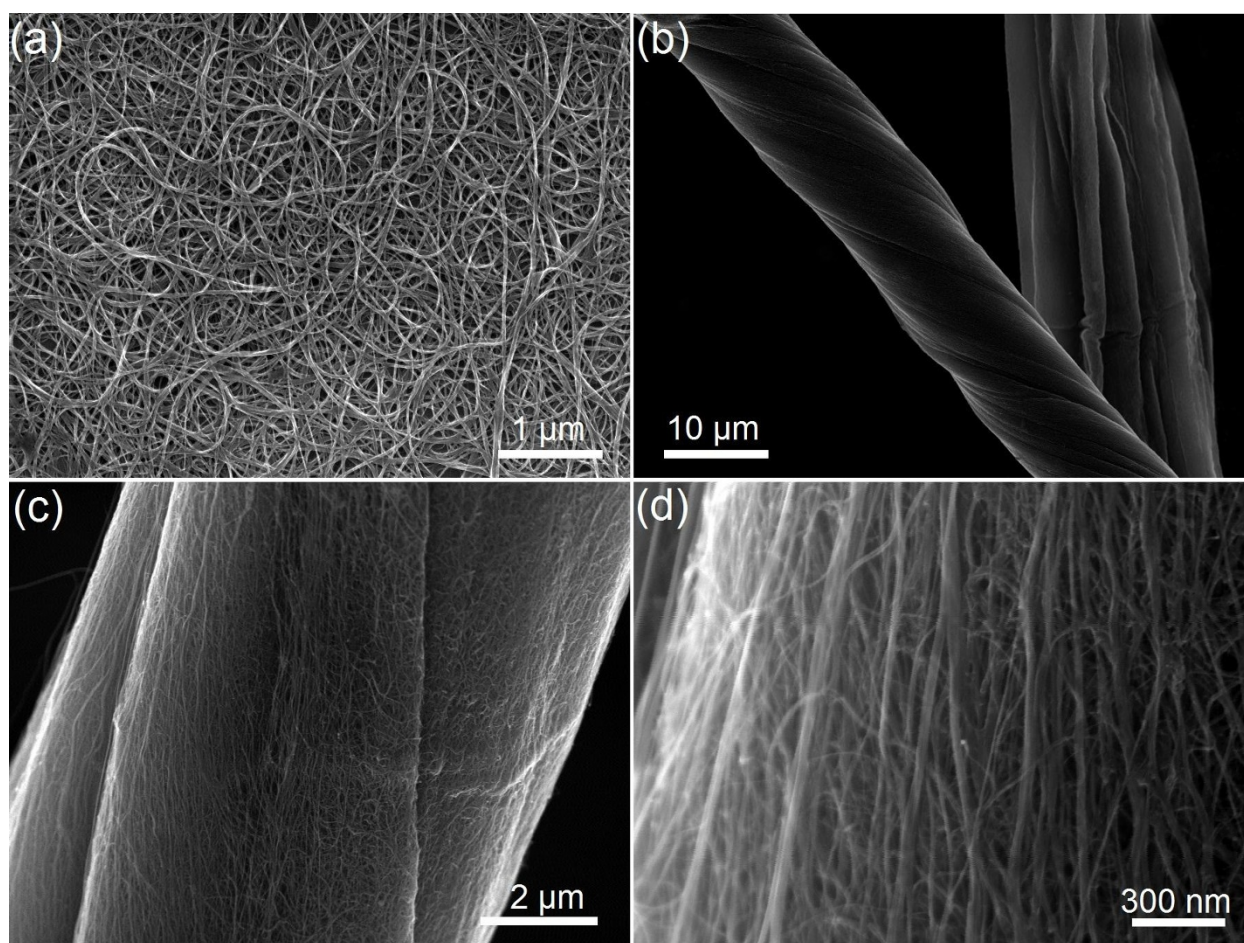


Figure 2 SEM images. (a) The single-walled CNT (SWNT) film and (b, c, d) a densified and twisted SWNT fiber.

process allowed one-step formation of continuous nanotube fibers.

Before solar cell assembly, the mechanical properties of the SWNT fibers are tested. Figure 3a shows typical stress-strain curves for three SWNT fibers before fracture. All the SWNT fibers fractured at the highest load. The tensile strength and Young's modulus of our SWNT fibers were measured in the range 0.8 to 1.0 GPa and 8 to 10 GPa, respectively. During loading to failure, the fibers, and hence the SWNT bundles, experienced two different strains, elastic strain and plastic strain, owing to slippage between aligned bundles and plastic deformation of individual nanotubes. Three different fracture morphologies were observed: (1) brittle fracture due to strong inter-bundle coupling (Figure 3b), (2) fan-shaped fracture surface due to fiber unwinding (Figure 3c), and (3) sliding of bundles due to weak inter-bundle coupling and small twist angle (approximately 11°) (Figure 3d).

The high tensile strengths of the SWNT fibers are consistent with their electrical conducting performance. Owing to the higher density, the conducting properties

of the twisted fibers are superior to the original fibers. Figure 4a shows the current density versus voltage curves of a typical SWNT fiber (approximately 1 cm long) before and after twisting. The current density is defined as the current per unit cross-sectional area of the SWNT fiber. The conductivity was enhanced featured with the resistivity reduced by approximately 40% from 9.7×10^{-4} to $5.5 \times 10^{-4} \Omega \cdot \text{cm}^{-1}$. Raman spectra at an excitation of 633 nm show high G-band intensity (I_G) and very low D-band intensity (I_D) of as-produced CNT network (black) and CNT fiber (red) in Figure 4b. The ratios of I_G/I_D are about 30, indicating high crystallization of CNT and negligible amorphous carbon. The two peak positions remain unchanged (D-band at $1,322 \text{ cm}^{-1}$ and G-band at $1,589 \text{ cm}^{-1}$), revealing an absence of optical absorption change during the fiber twisting process.

Because the SWNT fibers were of macroscopic lengths and provided 1D electrical conducting channels, photovoltaic tests have been performed on the heterojunction solar cells made from the fibers and n-Si. The SWNT

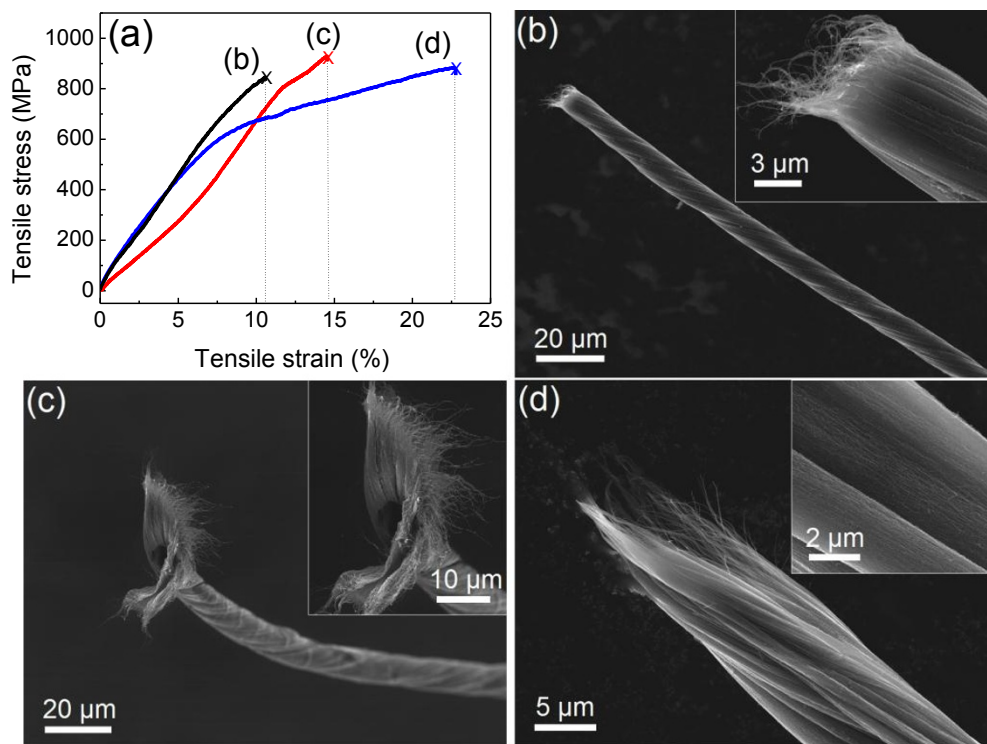


Figure 3 Mechanical properties of the single-walled CNT (SWNT) fibers. (a) Tensile stress-strain curves of three SWNT fibers. (b, c, d) SEM images of fractured SWNT fibers.

fiber/n-Si heterojunction was fabricated as illustrated in Figure 5a. An n-type Si (100) wafer (doping density, $2 \times 10^{15} \text{ cm}^{-3}$) with a 300-nm SiO_2 layer was patterned by photolithography and wet-etching to make a square window of 9 mm^2 . A back electrode of a Ti/Pd/Ag layer was used to ensure high-quality Ohm contact with the silicon. A SWNT fiber was then transferred to the top

of the patterned silicon wafer and naturally dried. To introduce a strong adhesion between the fiber and the wafer, a piece of transparent tape was coated on the fiber. Forward bias was defined as positive voltage applied to the SWNT fiber. The current-voltage data were recorded using a Keithley 2601 SourceMeter (Keithley Instruments, Inc., Cleveland, OH, USA). The

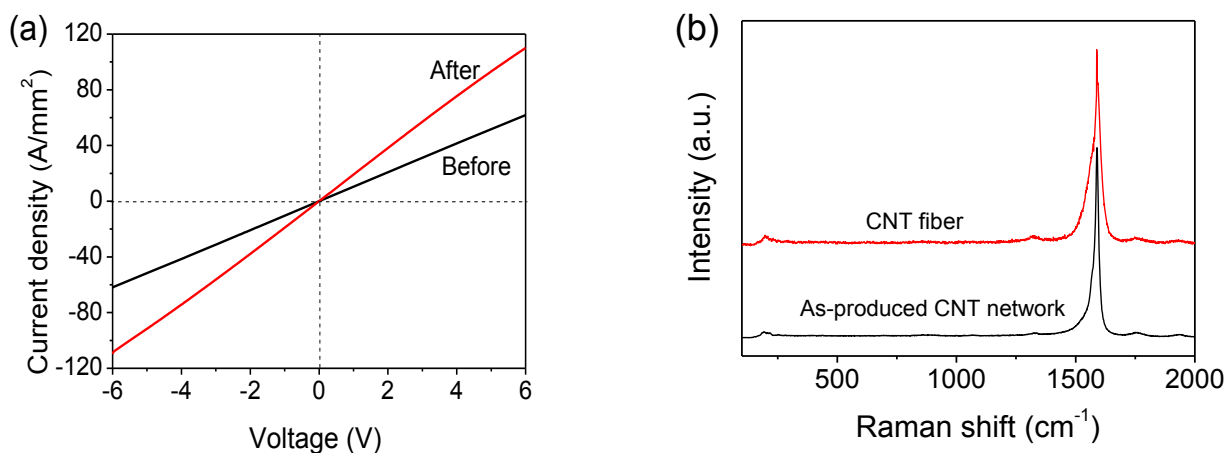


Figure 4 Conducting properties of the single-walled CNT (SWNT) fibers. (a) Current density-voltage curves of a SWNT fiber before and after twisting. (b) Raman spectra of as-produced CNT network and CNT fiber.

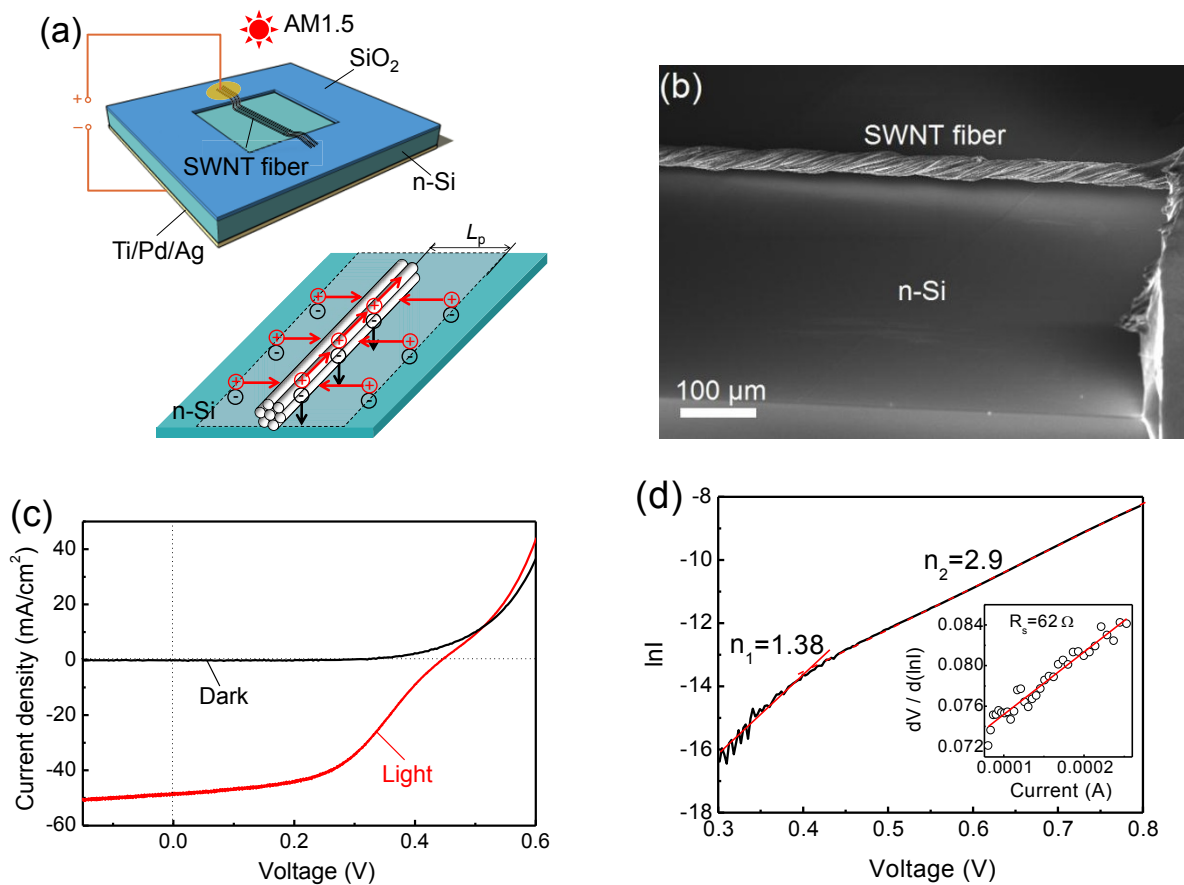


Figure 5 The single-walled CNT (SWNT) fiber/n-Si solar cell. (a) Device schematics of the SWNT fiber/n-Si solar cell. (b) SEM image of the SWNT fiber/n-Si junction. (c) Dark and light (AM1.5) J - V curves of the SWNT fiber/n-Si solar cell. (d) $\ln I$ - V plot and (inset) $dV/d(\ln I)$ plot.

solar devices were tested with a Newport solar simulator (Newport, Beijing, China) under AM1.5 condition.

As illustrated in the bottom panel of Figure 5a, the fiber acted as a hole collector to extract the photo-excited holes generated within the rectangle region (marked with a dashed line) defined by the minority diffusion length (L_p) (approximately 20 μm for n-Si at $2 \times 10^{15} \text{ cm}^{-3}$ doping level) of the silicon and the fiber length. Figure 5b shows a SEM image of the SWNT fiber/n-Si junction.

Figure 5c shows the measured current density-voltage (J - V) characteristics for a typical SWNT fiber/Si cell. Based on the J - V characteristics, the energy conversion efficiency (η) of the solar cell was estimated. The efficiency is defined by

$$\eta = j_{sc} \cdot V_{oc} \cdot FF / P_{in}$$

where J_{sc} is the short-circuit current density ($J_{sc} = I_{sc}/S$). Here, the nominal current density is defined as the current per unit projectional area ($S_n = \text{length} \times \text{diameter}$) of the SWNT fiber; the actual current density is

defined as the current per unit area when the minority diffusion in silicon is considered ($S_a = S_n + 2L_p \times \text{length}$). Correspondingly, the actual efficiency (η_a) and nominal efficiency (η_n) will be obtained. V_{oc} is the open-circuit voltage, P_{in} is the incident power density (100 mW/cm²), and FF is the fill factor, which is defined by the relation

$$FF = J_m \cdot V_m / J_{sc} \cdot V_{oc}$$

where ($J_m V_m$) is the maximum power point of the J - V characteristic of the solar cell.

Along with the other two tested cells, the photovoltaic performance of the three cells is summarized in Table 1. Initial tests have shown η_a of 2% to approximately 3% and η_n of 6% to approximately 10% at AM1.5, proving that SWNT fiber-on-Si is a potentially suitable configuration for making solar cells. Comparing sample #1 and sample #2 with different diameters in Table 1 the smaller diameter results in a smaller projectional area (S_n) and entire effective area (S_a), leading to a higher cell efficiency.

Table 1 Photovoltaic performance of the three SWNT fiber/n-Si solar cells.

Samples	Diameter (μm)	S_a (10^{-4} cm^2)	S_n (10^{-4} cm^2)	I_{sc} (μA)	V_{oc} (V)	FF (%)	η_a (%)	η_n (%)
#1	17.1	17.1	5.13	24.9	0.445	49.1	3.17	10.6
#2	29.8	21.1	8.95	33.8	0.475	40.1	3.07	7.19
#3	18.6	17.6	5.57	22.1	0.414	41.4	2.16	6.80

S_a , actual current density; S_n , nominal current density; I_{sc} , short-circuit current; FF, fill factor; η_a , actual efficiency; η_n , nominal efficiency; V_{oc} , open-circuit voltage.

As shown in Figure 5c, the V_{oc} and FF of the SWNT fiber/Si device are 0.445 V and 49.1%, respectively, which are comparable to the values for CNT film/Si cells [32]. The overall η_n of the fiber device (approximately 10.6%) is about 43% higher than that of the film device (approximately 7.4%). This disparity arose mainly from the different definition of the junction area for these two devices. In this fiber device, the η_a is 3.17% when the entire effective area is used instead of only the fiber projection area. It is worth mentioning that the size of the inter-bundle voids within a CNT film is $< 5 \mu\text{m}$ [32], which is substantially smaller than the L_p (20 μm). This implies that the SWNT bundles with an inter-spacing of $2 L_p$ will give the optimal charge collection. The cell efficiencies are expected to be further improved by acid doping [16].

Consistent with the characteristics of the 1D/2D junction, we note that the device only shows a moderate rectification ratio which is approximately 1,680 at ± 0.8 V, and a typical reverse current at -1.0 V is 250 nA. As shown in Figure 5d, at low forward voltages, the current follows an exponential dependence with ideality factor (n) equal to 1.38. At higher voltages, the current follows an exponential dependence with an ideality factor of 2.9. This variation corresponds to a transition between two regimes [33]: (1) the current is dominated by diffusion and generation-recombination outside the space charge region ($n = 1$), and (2) the high-injection regime, where the density of the minority carrier is comparable with that of the majority ($n = 2$). A $dV/d(\ln I)$ - I plot (Figure 5d, inset) is used to analyze the current-voltage characteristics when the series resistance (R_s) begins to dominate, yielding a R_s of approximately 62 Ω .

The 1D nature of the SWNT fiber offers a tremendous opportunity for exciton dissociation. SWNTs in the devices are involved in multiple processes including hole collecting and transporting. Despite its opaque feature and the relatively small interfacial area for charge separation, the SWNT fiber provides many 1D paths, forming a conducting channel for charge transport.

The devices present a great potential for use as photovoltaic solar cells and light sensors. In addition to enhancing photovoltaic conversion efficiency, the incorporation of the robust SWNT fibers can potentially improve the mechanical and environmental stability of the devices.

Conclusions

To conclude, we have demonstrated the photovoltaic properties of the SWNT fiber/Si heterojunction and revealed that SWNTs can be used as efficient hole collectors. The SWNT fiber/n-Si solar cell studied here represents an addition to the CNT film/n-Si counterparts reported by us previously. The photovoltaic devices also show excellent structural stability due to the use of strong, environmentally benign CNT fibers.

Acknowledgements

This work was supported by the National Science Foundation of China (50972067) and the Research Fund for Doctoral Program of Education Ministry of China (20090002120019 and 20090002120030).

Author details

¹Key Laboratory for Advanced Materials Processing Technology, Ministry of Education and Department of Mechanical Engineering, Tsinghua University, Beijing, 100084, People's Republic of China ²Department of Advanced Materials and Nanotechnology, College of Engineering, Peking University, Beijing, 100871, People's Republic of China ³Center for Nano and Micro Mechanics, Tsinghua University, Beijing, 100084, People's Republic of China

Authors' contributions

YJ carried out the solar cell assembly and test, and drafted the manuscript. XL participated in the solar cell assembly. PL prepared the carbon nanotube films. AC, DW, and HZ conceived of the study and participated in its design and coordination. JW and KW participated in the data analysis. All authors read and approved the final manuscript.

Competing interests

The authors declare that they have no competing interests.

Received: 17 October 2011 Accepted: 17 February 2012

Published: 17 February 2012

References

1. Avouris P, Freitag M, Perebeinos V: Carbon-nanotube photonics and optoelectronics. *Nat Photon* 2008, **2**:341-350.
2. Zhu HW, Wei JQ, Wang KL, Wu DH: Applications of carbon materials in photovoltaic solar cells. *Sol Energy Mater Sol Cells* 2009, **93**:1461-1470.
3. Zhu HW, Wei BQ: Assembly and applications of carbon nanotube thin films. *J Mater Sci Tech* 2008, **24**:447-456.
4. Wei JQ, Jia Y, Shu QK, Gu ZY, Wang ZC, Zhuang DM, Zhang G, Wang ZC, Luo JB, Cao AY, Wu DH: Double-walled carbon nanotube solar cells. *Nano Lett* 2007, **7**:2317-2321.
5. Jia Y, Wei JQ, Wang KL, Cao AY, Shu QK, Gui XC, Zhu YQ, Zhuang DM, Zhang G, Ma BB, Wang LD, Liu WJ, Wang ZC, Luo JB, Wu DH: Nanotube-silicon heterojunction solar cells. *Adv Mater* 2008, **20**:4594-4598.
6. Zhou H, Colli A, Ahnood A, Yang Y, Rupasinghe N, Butler T, Haneef I, Hiralal P, Nathan A, Amarantunga GAJ: Arrays of parallel connected coaxial multiwall carbon nanotube amorphous silicon solar cells. *Adv Mater* 2009, **21**:3919-3923.

7. Arena A, Donato N, Saitta G, Galvagno S, Milone C, Pistone A: **Photovoltaic properties of multi-walled carbon nanotubes deposited on n-doped silicon.** *Microelectronics J* 2008, **39**:1659-1662.
8. Li ZR, Kunets VP, Saini V, Xu Y, Dervishi E, Salamo GJ, Biris AR, Biris AS: **SOCl₂ enhanced photovoltaic conversion of single wall carbon nanotube/n-silicon heterojunctions.** *Appl Phys Lett* 2008, **93**:243117.
9. Li ZR, Kunets VP, Saini V, Xu Y, Dervishi E, Salamo GJ, Biris AS: **Light-harvesting using high density p-type single wall carbon nanotube/n-type silicon heterojunctions.** *ACS Nano* 2009, **3**:1407-1414.
10. Ong PL, Euler WB, Levitsky IA: **Hybrid solar cells based on single-walled carbon nanotubes/Si heterojunctions.** *Nanotechnol* 2010, **21**:105203.
11. Li CY, Li Z, Zhu HW, Wang KL, Wei JQ, Li X, Sun PZ, Zhang H, Wu DH: **Graphene nano-"patches" on carbon nanotube network for highly transparent/conductive thin film applications.** *J Phys Chem C* 2010, **114**:14008-14012.
12. Jia Y, Li PX, Wei JQ, Cao AY, Wang KL, Li CL, Zhuang DM, Zhu HW, Wu DH: **Carbon nanotube films by filtration for nanotube-silicon heterojunction solar cells.** *Mater Res Bull* 2010, **45**:1401-1405.
13. Shu QK, Wei JQ, Wang KL, Zhu HW, Li Z, Jia Y, Gui XC, Guo N, Li XM, Ma CR, Wu DH: **Hybrid heterojunction and photoelectrochemistry solar cell based on silicon nanowires and double-walled carbon nanotubes.** *Nano Lett* 2009, **9**:4338-4342.
14. Shu QK, Wei JQ, Wang KL, Song S, Guo N, Jia Y, Li Z, Xu Y, Cao AY, Zhu HW, Wu DH: **Efficient energy conversion of nanotube/nanowire-based solar cells.** *Chem Commun* 2010, **46**:5533-5535.
15. Jia Y, Cao AY, Bai X, Li Z, Zhang LH, Guo N, Wei JQ, Wang KL, Zhu HW, Wu DH: **Achieving high efficiency silicon-carbon nanotube heterojunction solar cells by acid doping.** *Nano Lett* 2011, **11**:1901-1905.
16. Jia Y, Cao AY, Li PX, Gui XC, Zhang LH, Wei JQ, Wang KL, Zhu HW, Xu Y, Wu DH: **Encapsulated carbon nanotube-oxide-silicon solar cells with stable 10% efficiency.** *Appl Phys Lett* 2011, **98**:133115.
17. Zhang LH, Jia Y, Wang SS, Li Z, Ji CY, Wei JQ, Zhu HW, Wang KL, Wu DH, Shi EZ, Fang Y, Cao AY: **Carbon nanotube and CdSe nanobelt Schottky junction solar cells.** *Nano Lett* 2010, **10**:3583-3589.
18. Li XM, Zhu HW, Wang KL, Cao AY, Wei JQ, Li CY, Jia Y, Li Z, Li X, Wu DH: **Graphene-on-silicon Schottky junction solar cells.** *Adv Mater* 2010, **22**:2743-2748.
19. Li X, Li CY, Zhu HW, Wang KL, Wei JQ, Li XM, Xu EY, Li Z, Luo S, Lei Y, Wu DH: **Hybrid thin films of graphene nanowhiskers and amorphous carbon as transparent conductors.** *Chem Commun* 2010, **46**:3502-3504.
20. Pereira LFC, Rocha CG, Latgé A, Coleman JN, Ferreira MS: **Upper bound for the conductivity of nanotube networks.** *Appl Phys Lett* 2009, **95**:123106.
21. Behabtu N, Green MJ, Pasqualia M: **Carbon nanotube-based neat fibers.** *Nanotoday* 2008, **3**:24-34.
22. Zhu HW, Xu CL, Wu DH, Wei BQ, Vajtai R, Ajayan PM: **Direct synthesis of long single-walled carbon nanotube strands.** *Science* 2002, **296**:884-886.
23. Li YL, Kinloch IA, Windle AH: **Direct spinning of carbon nanotube fibers from chemical vapor deposition synthesis.** *Science* 2004, **304**:276-278.
24. Motta M, Moisala A, Kinloch IA, Windle AH: **High performance fibres from 'dog bone' carbon nanotubes.** *Adv Mater* 2007, **19**:3721-3726.
25. Koziol K, Vilatela J, Moisala A, Motta M, Cuniff P, Sennett M, Windle A: **High-performance carbon nanotube fiber.** *Science* 2007, **318**:1892-1895.
26. Vilatela JJ, Windle AH: **Yarn-like carbon nanotube fibers.** *Adv Mater*, doi: 10.1002/adma.201002131.
27. Zhang M, Atkinson KR, Baughman RH: **Multifunctional carbon nanotube yarns by downsizing an ancient technology.** *Science* 2004, **306**:1358-1361.
28. Ericson LM, Fan H, Peng H, Davis VA, Zhou W, Sulpizio J, Wang YH, Booker R, Vavro J, Guthy C, Parra-Vasquez ANG, Kim MJ, Ramesh S, Saini R, Kittrell C, Lavin G, Schmidt H, Adams WW, Billups WE, Pasquali M, Hwang WH, Hauge RH, Fischer JE, Smalley RE: **Macroscopic, neat, single-walled carbon nanotube fibers.** *Science* 2004, **305**:1447-1450.
29. Zhang XF, Li QW, Tu Y, Li Y, Coulter JY, Zheng LX, Zhao YH, Jia QX, Peterson DE, Zhu YT: **Strong carbon-nanotube fibers spun from long carbon-nanotube arrays.** *Small* 2007, **3**:244-248.
30. Zhang XF, Li QW, Holesinger TG, Arendt PN, Huang JY, Kirven PD, Clapp TG, DePaula RF, Liao XZ, Zhao YH, Zheng LX, Peterson DE, Zhu YT: **Ultrastrong, stiff, and lightweight carbon-nanotube fibers.** *Adv Mater* 2007, **19**:4198-4201.
31. Li X, Li CY, Li XM, Zhu HW, Wei JQ, Wang KL, Wu DH: **Force- and light-controlled electrical transport characteristics of carbon nanotube bulk junctions.** *Chem Phys Lett* 2009, **481**:224-228.
32. Li Z, Jia Y, Wei JQ, Wang KL, Shu QK, Gui XC, Zhu HW, Cao AY, Wu DH: **Large area, highly transparent carbon nanotube spiderwebs for energy harvesting.** *J Mater Chem* 2010, **20**:7236-7240.
33. Sze SM, Ng KK: *The Physics of Semiconductor Devices*. 3 edition. New York: Wiley Interscience; 2007.

doi:10.1186/1556-276X-7-137

Cite this article as: Jia et al.: Strong, conductive carbon nanotube fibers as efficient hole collectors. *Nanoscale Research Letters* 2012 **7**:137.

Submit your manuscript to a SpringerOpen[®] journal and benefit from:

- Convenient online submission
- Rigorous peer review
- Immediate publication on acceptance
- Open access: articles freely available online
- High visibility within the field
- Retaining the copyright to your article

Submit your next manuscript at ► springeropen.com